Final Flotation Waste Kinetics of Sintering at Different Heating Regimes

Mira Cocić[1*)], Mihovil Logar[2], Branko Matović[3], Snežana Dević[4], Tatjana Volkov – Husović[5], Saša Cocić[6], Viša Tasić[7]

[1]University of Belgrade, Technical Faculty in Bor, VJ 12, 19210 Bor, Serbia
[2]University of Belgrade, Faculty of Mining – Geology, Belgrade, Serbia
[3]University of Belgrade, Vinca Institute of Nuclear Sciences, Materials Science Laboratory, Belgrade, Serbia
[4]Institute IMS Belgrade, Belgrade, Serbia
[5]University of Belgrade, Faculty of Technology and Metallurgy, Belgrade, Serbia
[6]Reservoir Minerals Inc.
[7]Mining and Metallurgy Institute Bor, Bor, Serbia

Abstract:

In the copper extraction, especially during the process of flotation enrichment and the pyrometallurgical processing, the waste materials that represent huge polluters of environment are being generated. In order to examine the application of Final flotation waste (FFW) in the manufacturing of new materials from the glass-ceramic group phase and mineral composition were examined as well as thermal properties. FFW kinetics of sintering has been tested at different dyamics (1^oC/min, 29^oC/min and 43^oC/min), in order to find the optimum conditions for sintering with a minimum amount of energy and time consumption. The samples were examined using: X-ray diffraction, X-ray fluorescence analysis, SEM (Scanning Electron Microscopy) and thermal microscopy. The best results for the production of glass ceramic materials were obtained during the sintering at heating regime of 29^oC/min.
Keywords: *Final flotation waste, Kinetics of sintering, Heating rate, Particle size distribution, Glass ceramics,*

1. Introduction

Production of copper in the Copper Smelting Plant Bor is a complex and long process with the generation and by-products such as flash furnace slags, converter slag, and anode refining slag. Since the processing cycle is closed, converter slag returns to further processing in the flash furnace. Also, anode refining slag returns to the converters for further processing. The slag formed by melting in the smelting plant is the only waste that is disposed of in a landfill. The basic components of waste smelter slag are FeO, Fe_2O_3 and SO_2, with small amounts of Al_2O_3, CaO and MgO [1-3].

The smelter slag is further processed with the aim of complete valorization. At the beginning, the slag is chopped (grin size below 12 mm) and then grinded, first in the mill with rods (up to 2 mm – 3 mm), then in the ball mill (60 % of the grain size finer than 74 μm). The

---

*) **Corresponding author**: mcocic@tf.bor.ac.rs

product of grinding is subjected to the flotation. As a result of flotation process, copper concentrate is extracted in the form of pulp. Waste material from the flotation process is transported to the thickeners and after thickening deposited in the flotation tailings. Deposits of FFW and slag discarded from the smelting furnaces contaminate large areas of soil and represent permanent source of water and air pollution [2-5]. These technogenic wastes are heterogeneous, because the copper ore has the different physical and chemical properties [2-4].

According to the data taken from the Copper Smelting Plant Bor, Serbia, the total amount of waste smelter slag deposited in the landfill is approximately 16 million tons [2-4]. In addition to already deposited slag, the copper smelter produces 700 - 1000 tons of slag per day, depending on the work regime, with an average copper content of 0.75 %. [2-4]. Mass of flotation tailings are estimated at around 27 million tonnes, with an average copper content of about 0.2-0.4 % [2-4]. According to the fact that those are materials of ferro silicate composition, a possibility of their valorization is of great significance, not only because of the industrial waste quantity reduction but also as a potential resource for launching of the new technology initiatives [2-4].

The glass ceramic materials and glass rich with iron from industrial wastes have been investigated by many authors. Vitrification of a hazardous iron-rich waste from copper [6, 7] and zinc industry [8], provide chemically stable glass-ceramic materials with significantly better performance compared to traditional ceramic and natural building materials for paving (marbles and granites).

In the last two decades, there have been numerous studies of hazardous waste from the flotation of copper ores investigating not only the recovery of valuable metals, but also usability of hazardous waste as a raw material in cement industry [9], fillers, abrasives, tiles, etc... [10]. The recycling and utilization of jarosite formed in the extraction of Zn were investigated by Asokana et al. [11-13]. They investigated the solidification / stabilization (S / S) and sintering of jarosite converted into products that can be used as a building material: mixing clay [11], sand [12] or with the rest of the combustion of coal [13]. Also, hydrometallurgical process for treating the hazardous jarosite, by leaching with aqueous NH_4Cl and then the NaOH solution, is proposed by Yu et al. [14], not only for detoxifying the residue, but also for recovering the valuable metal contained components. The black glasses with good mechanical and chemical properties was investigated by Romero and Rincon [15] by recycling goethite (FeOOH) - from hydrometallurgical industrial waste of zinc with added glass cullet and dolomite. Recycling of hazardous and non-hazardous wastes from India for the development of alternative building materials as a substitute for traditional materials (such as bricks, blocks, tiles, aggregates, ceramics, cement, lime, soil, wood and paint) was discussed by Asokan et al. [16]. In reference [17] coal fly ash is proposed as a raw material for the production of glass-ceramics with high-performance. A novel type of ceramic material was produced by mixing sago waste ash from the sago processing industry in Indonesia with clay by Aripina et al. [18]. In addition, fiber glass strip with good mechanical capability of binding was obtained by vitrification (at 1350 1500°C) of industrial waste of Reggio Emilia and sludge from the lagoon of Venice, Italy [19].

Vitrification was selected as the most fitting technology for treatment the toxic waste under investigation by many authors [6-8, 11, 13, 18-21]. During the vitrification process significant amounts of toxic organic and inorganic chemical compounds could be eliminated, and at the same time, the metal species are immobilized as they become an integral part of the glass matrix [7]. Vitrification process i.e. reduction in porosity by a viscous silicate-based liquid is the ultimate purpose of firing of many silicate systems. Viscous silicate liquid is formed at firing temperatures acting as a binder. The viscosity of liquid phase, has to be low enough that densification of the body has to be accomplished within a given time interval without deformation. Relative and absolute speeds i.e. sintering kinetics of these two

processes (densification and deformation), are mostly defined by temperature, composition and grain size [22].

The different heating regimes cause different effects on sample behavior during the sintering and application of FFW. The aim of this work is to find the optimal conditions of glass-ceramic synthesis using FFW as the raw material. Considering the fact that sintering is taking place in presence of liquid phase, the risk with the application of 'sharp' dynamic regimes is rapid development of liquid phase, followed by the rapid drop of viscosity that can cause deformation. On the other hand, a slow heating process involves higher production costs.

2. Experimental
2.1. Material and methods

FFW was sampled at the output of flotation just before transport to the landfill. FFW sample is thoroughly analyzed in order to examine the possibility of its application for the synthesis of ceramic glass and to determine optimal temperature regimes for sintering. Phase composition was determined by X-ray powder diffraction. The diffraction patterns were obtained using Siemens D500 diffractometer by applying CuKα radiation (λ = 1,54184 Å) and Ni-filters, with a current of 20 mA and a voltage of 35 kV in the range from 5 to 85° (2θ) with a step of 0.02° and exposure of 0.5 s per step. The phases ratio has been determined by Powder Cell (PCW) using structural models of magnetite [23], fayalite [24] and hematite [25]. The chemical composition was determined by using X-ray fluorescent analysis (PANalytical AXIOS XRF Spectrometer) and JEOL JSM-6610LV Scanning Electron Microscope which is connected with X-Max Energy Dispersive Spectrometer. Samples were covered with carbon using BALTEC-SCD-005 Sputter coating device and recorded under conditions of high vacuum. Grain size was determined by microscope using digital image analysis (MAUD software). Granulometric fractions are extracted by Andersen decantation method.

To test the thermal properties of the FFW, powder sample is dry pressed under a pressure of 60 MPa in a mold (cube 4x4x4 mm). Intervals of sintering, softening and melting of the cube samples were determined by thermomicroscope Carl Zeiss - Jena equipped with video system and digital camera (Canon PRO-1) for the automatic recording and monitoring. The changes in the sample were monitored and recorded in the temperature range between 20°C and 1500°C. The heating regimes were 1°C/min, 29°C/min and 43°C/min. The temperature of the sample is measured by PtPt-Rh thermocouple. Assuming expansion isotropy, the curve of volume change as function of temperature was obtained by measurement the surface of visible side of sample. The melting temperature was determined when sample reached the hemisphere shape.

3. Results and discussion
3.1. Characterization of the FFW

Tab. I shows chemical and phase composition of FFW being calculated based on identification done by X-ray powder diffraction analysis with the use of Rietveld analyses (Fig. 1), and from chemical composition (determined by RFA) using theoretical, stoichiometric formulas of magnetite and fayalite. During the process, it was strived to fit phase's composition into final measured density of FFW according to theoretical density. Fayalite stoichiometric formula has been calculated allowing MgO to be present in the composition. It was obtained that FFW is composed of: fayalite 40 %, magnetite 25 % and

glass 35 % that represent significant basis for production of glass-ceramics. Having in mind that x-ray system "cannot see" amorphous material (glass) and exact composition of olivine stage is not known, limit of the fayalite content is not precise. The shown content of the glass is recalculated on 100 %. Its density is calculated approximately using program from the website [26]. Results are in accordance to the results obtained by the chemical composition.
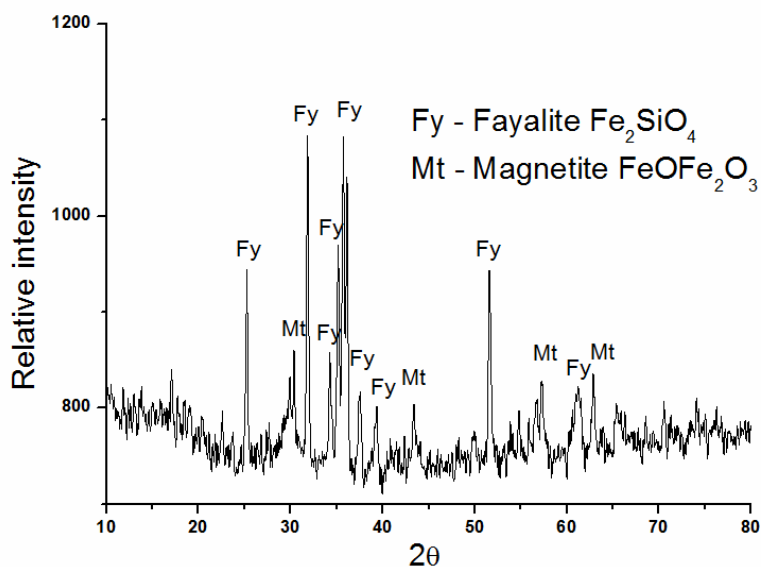

Fig. 1. X-ray powder diffraction diagram of FFW [3].

Tab. I Chemical and phase compositions of FFW [3].

The chemical composition of FFW		The phases participation			The calculated glass chemical composition
		Magnetite	Fayalite	Glass	
	wt-%	$FeOFe_2O_3$	$(Fe^{2+}_{1.72},Mg_{0.28})_2 SiO_4$		
SiO_2	34.27	-	13.64	20.63	59.22
TiO_2	0.36	-	-	0.36	1.03
Al_2O_3	4.89	-	-	4.89	13.93
Fe_2O_3	52.10	25.34	25.97	0.78	2.94
Mn_3O_4	0.07	-	-	0.07	0.20
MgO	0.79	-	0.79	0.00	0.00
CaO	4.58	-	-	4.58	13.05
Na_2O	0.31	-	-	0.31	0.88
K_2O	1.22	-	-	1.22	3.48
P_2O_5	0.07	-	-	0.07	0.20
SO_3	0.50	-	-	0.50	1.42
CuO	0.49	-	-	0.49	1.40
ZnO	0.79	-	-	0.79	2.25
sum %	100.44	25.34	40.40	34.70	100.00
Density (g/cm^3)	3.65	5.15	4.39	2.60	

3.2. Granulometric distribution of ground FFW

Diagram of grain size distribution (Fig. 2) points out that 75 % of the sample is taken by the granulometric classes up to 10 μm, while classes over 10 μm are there with 25 %. Total grain size distribution does not have symmetrical diagram, so we can conclude that its structure is composed of two virtual granulometric populations.
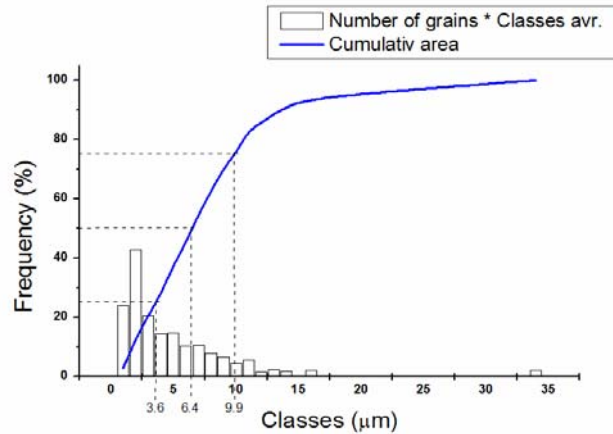

Fig. 2. Diagram of the granulometric distribution of ground FFW [3].

The boundaries of grains were determined by deconvolution of the total granulometric distribution presented by the Gaussian model (Fig. 3). Optimal results for the two superposed distribution were obtained, with a maximum grain frequency at 1.3 μm for one distribution and 4.3 μm for another. From the Fig. 3, it is obvious that the grain size distribution of populations below the limit of 2.5 μm predominantly contained particles of diameter about 1.3 μm and overhead particle diameter is about 4.5 μm. Assuming the known density of FFW, the rate of deposition for particles with size of 2.5 μm is calculated by Stokes law. The separation of grains is carried out in an aqueous medium.
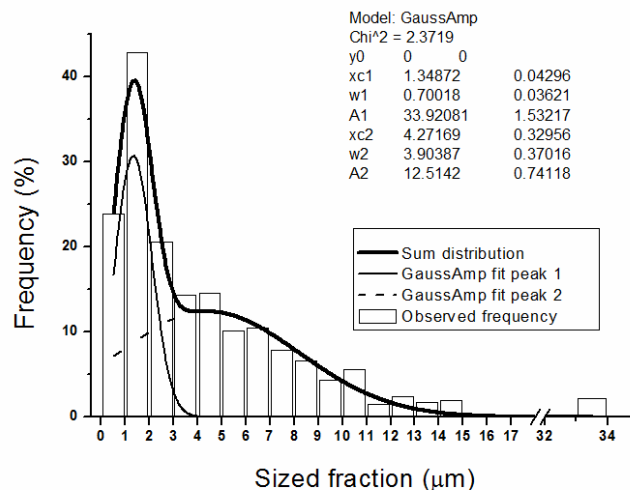

Fig. 3. Diagram of the bimodal granulometric distribution of ground FFW [3].

3.3. The kinetics sintering at different heating regimes of FFW

Measuring slag sample size change in function of time, due to heating on thermo microscope at different heating regimes, diagrams of sintering kinetics FFW were obtained,

Figs. 4 - 6. Points on diagrams are experimental data. Curves are differentials of sintering speed, that is, increment of density in unit of time $d\rho/dT$ in determined temperature interval that fit properly by Gaussian distribution. Maximums of their sums provide integral of differential. Starting density of the sample was 2.7 g/cm^3.

By heating in very slow regime (1°C/min) (Fig. 4), there are two separated sintering intervals spotted. The first sintering interval appears between 860°C and 995°C. Maximal density increment occurs at 965°C, 14 minutes after the start of sintering (as shown in Fig. 4). The second interval of sintering is taking place at the temperature between 1010 and 1050°C with maximum at 1040°C, 60 minutes later. At the temperature of 1050°C sintering is being finished and maximum density of 4.2 g/cm^3 has been achieved. It is assumed that two separated intervals is consequence of different reaction speeds of the particles of different sizes. The aim was to maintain constant temperature during as long as possible time frame what provides the biggest contribution to volume change. After 14 minutes, maximum speed of sintering is reached by fraction of 1.4 µm grain diameter and after 60 minutes maximum speed is being reached by fraction of grain diameter 4.3 µm. Times intervals of 14 and 60 min are real whilst the granulations of 1.4 µm and 4.3 µm are theoretically calculated.
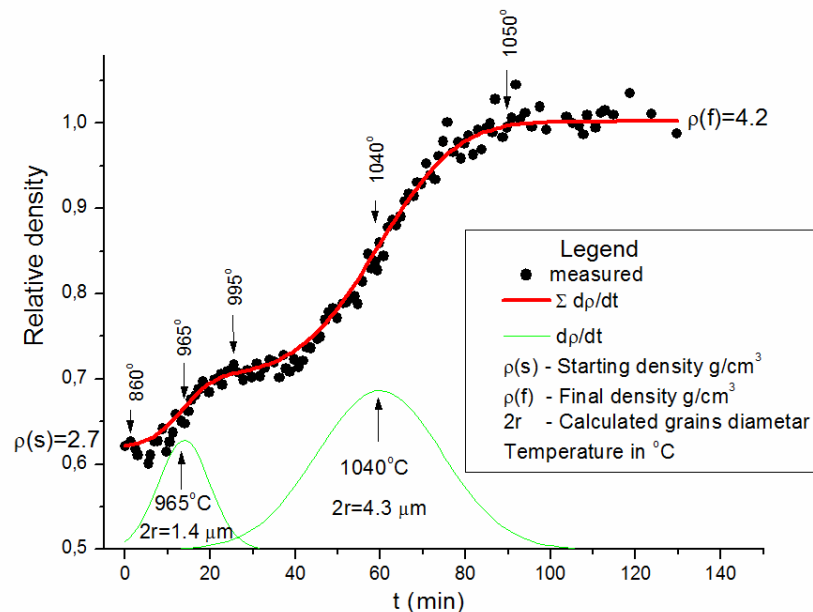

Fig. 4. Sintering kinetics diagram of FFW 1°C/min (d˜dt not in scale with relative density) [3].

According to classical theory [22], grain size for starting sintering speed is being calculated using Eq. (1):

$$\Delta V/V_o = 9\ \gamma/4\eta r * t \qquad (1)$$

where is:

    $\Delta V/V_o$ – relative density,
    ΔV – change the volume (which is proportional to the time), ($\Delta V = V - V_o/V_o$)
    V_o – initial volume
    γ – surface tension (N/m),
    η – viscosity (Pa s)
    r – radius of the particles (m)
    t – time (s)

Viscosity is calculated according to "Glass-viscosity calculation based on global statistical modeling approach" [27], while the surface tension is calculated based on: "Surface tension calculation of glass melts at 1400°C" [28]. Providing that the FFW glass composition

is a bit out of the applied software limits, the extrapolation has been necessary. Nevertheless, the calculated surface tension of 1 mN/m and viscosity of 106 Pas is expected for temperatures below 1000°C.

Having in mind that Equation (1) applies in area of linear increment of density with time, obtained accordance is approximate but as it will be shown later it has been confirmed by other experiment (Fig. 7).

When regime of heating is 29°C/min (Fig. 5), two sintering intervals are being recognized as well. However, borderline of the ending of sintering interval I and at beginning of sintering interval II is not clearly expressed. First sintering interval begins at 935°C and it reaches maximum speed of sintering at 970°C. At 990°C first sintering interval ends where second sintering interval begins, id est. there is an overlap. Maximum speed of sintering at interval II is at 1030°C. At 1080°C sintering is finished and maximum relative density achieved.
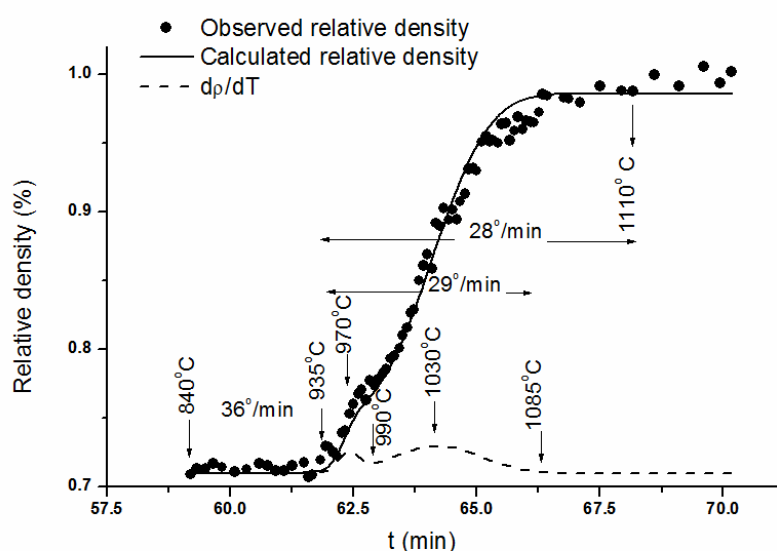

Fig. 5. Sintering kinetics diagram of FFW 29° C/min (d ~ dt not in scale with relative density).

Liquid phase that came out of small grain fraction during the first interval of sintering provides its contribution to starting of large grain size fractions sintering. Reduction of the first part of volume happens in the first sintering interval, while the second part of volume reduction comes from porosity of large grain fraction. Hence, sintering until beginning of second sintering interval is regrouping of particles since porosity of large grain fraction is not being changed. Inside large pores small grains are being mutually sintered but also react with large grains. Porosity between small grains during the first interval of sintering is being minimized. When the second sintering interval begins, reduction of volume starts by disappearance of pores between large grains. Contribution to the part of sintering is given by already existent liquid phase produced by the small grains. If there was no small fraction, sintering would have started later.

At fastest regime of heating of 43°C/min (Fig. 6), beginning of density increment, i.e. beginning of sintering is at the 920°C. The biggest density increment (shrinkage rate) at this regime is being achieved at 1005°C, when maximum shrinkage rate is reached, and the end of sintering is at 1075°C. Hence, the total sintering time at this regime is only 3.6 minutes.

The results of testing the thermal characteristics of FFW determined by thermo microscope at different heating regimes are given in Tab. II. In the case that the heating mode is slow enough, there are two intervals of sintering, clearly separated in the heating mode of

1°C/min. At the higher heating rate (43°C/min), the development of the liquid phase is very fast so, only one interval of sintering appears.
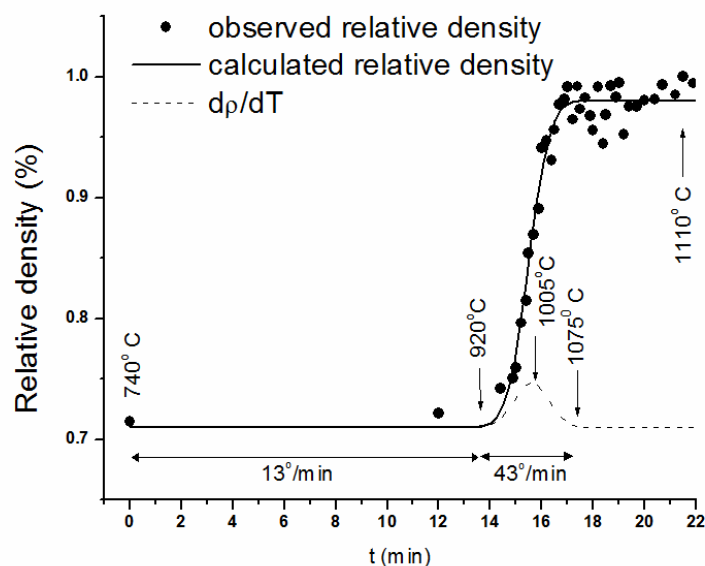

Fig. 6. Sintering kinetics diagram of FFW 43°C/min (dρ/dt not in scale with relative density).

Tab. II Experimental results obtained by thermo microscope.

	FFW		
Heating mode	1°C/min	29°C/min	43°C/min
I interval of sintering	t (°C)	t (°C)	t (°C)
Beginning of sintering	920°C	935°C	920°C
Temperature at the maximum sintering rate dr/dt	940°C	970°C	1005°C
End of sintering	965°C	990°C	1075°C
II interval of sintering			
Beginning of sintering	1010°C	990°C	
Temperature at the maximum sintering rate dr/dt	1040°C	1030°C	
End of sintering	1050°C	1085°C	
Total time of sintering	85 min	5.2 min	3.6 min

3.4. The sintering kinetics of two specimens with different granulation

Having in mind that that two mutually segregated sintering intervals are a consequence of unequal speed of reaction of particles of different sizes, using Andersen method of decantation, two granulometric fractions have been separated up to 2.5μm and over 2.5μm. Two samples bodies of different granulometric fraction were prepared. Shrinkage rate, times of sintering and plastic deformation have been experimentally analyzed on thermo microscope, at heating regime of 1°C/min. Figure 7 shows the diagram of sintering kinetics of two granulations. It is obvious that grain size distribution below 2.5 μm is being sintered at the temperature interval of 850°C and 995°C. Fraction over 2.5 μm starts sintering at temperature of 1030-1040°C and ends at 1100°C. Within temperature interval of 1100-1160°C, volume and density stay constant. At the temperature of 1160°C, yielding point
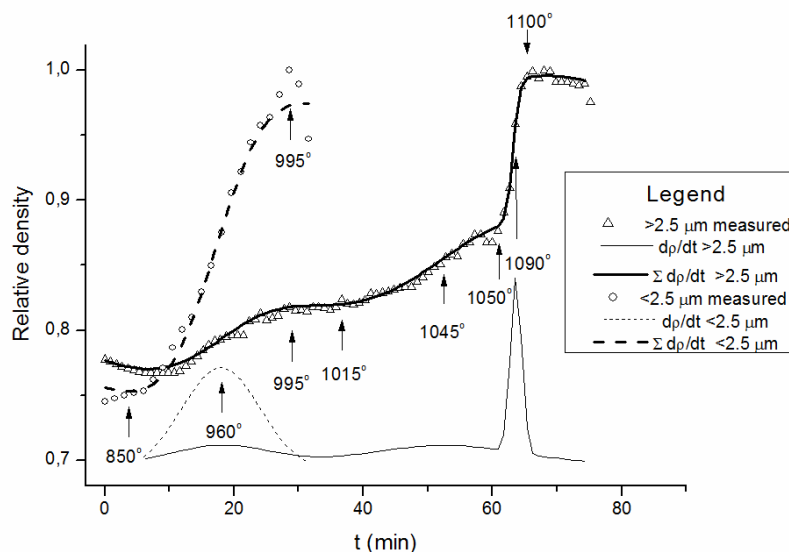
appears followed by increase of the sample volume.

Fig. 7. Sintering kinetics FFW - Two specimens of different grain size (dρdt not in scale with relative density).

By segregation of large grain fraction of FFW, reactivity of particles is much smaller, so sintering temperatures will be higher. Since the same material was testing, viscosity and surface tension are also the same: difference in sintering temperature is obviously the consequence of grain size. It can be explained by the fact that smaller grains due to higher specific surface are more reactive influencing that sintering can start at lower temperature.

By comparing the diagrams in Fig. 4 and 7, it can be noticed that the temperatures at the beginning and at the end of sintering are very similar. The first sintering interval of the entire sample FFW (Fig. 4.) is almost identical with the sintering temperatures of the sample with the fine-grained granulation (<2.5 m). The second sintering interval of the entire sample of FFW shows a lower starting and ending temperatures of sintering compared to the sample with coarse grains (> 2.5 m). This is due to the absence of fine-grained fractions. At lower temperatures fine particles crossing in the liquid phase. Capillary forces reformat particles and stimulate their softening on contacts, which stimulates shrinking and thickening.

3.7. Synthesis of glass ceramics

By sintering the pressed glass frit of FFW at $1150^{\circ}C$ (4h) and $1480^{\circ}C$ (6h), the glass-ceramics were obtained. The diffraction patterns in Fig. 8 shown that obtained glass ceramics are composed of hematite and glass phases. Namely, the magnetite from FFW transforms in hematite during the sintering due to the strong oxidation. Also, fayalite transforms in amorphous glass.

Fig. 9 presents the two glass-ceramics microstructures composed of glass and hematite crystals formed at different temperature. At $1150^{\circ}C$ the content of hematite is 32 %. The crystals are anhedral, rarely subhedral, with diameter generally below 10 microns. At $1480^{\circ}C$ viscosity decreases and the glass starts to flow. Therefore the glass surface is exposed to oxidation in the highest degree and growing rate of hematite becomes faster, leading to the formation of larger euhedral crystals, whose content reaches 44 %. By controlled thermal treatment ceramic material is obtained. The growth of crystal size of hematite is depended on by temperature [3, 7] and the duration of thermal treatment, which means that the content and size of hematite crystals can be controlled.
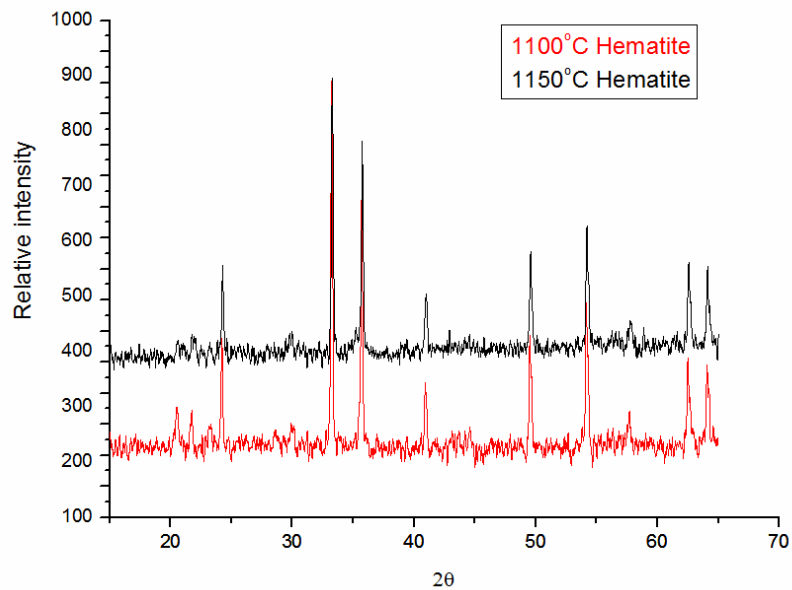
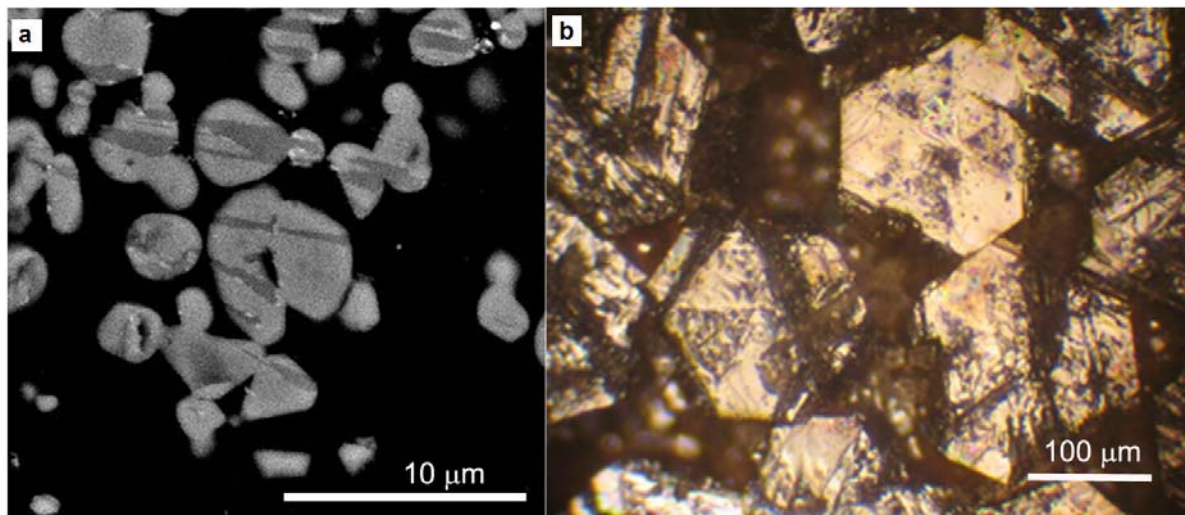**Fig. 8.** X-ray powder diffraction diagrams [3].

Fig. 9. Microstructure of glass ceramics: a) 1150°C (4h) (SEM), b) 1480°C (6h) (Optical Microscopy).

4. Conclusion

The aim of this study was to analyze the parameters that are of great significience for the control of technological processes of glass-ceramics production from FFW. Two parameters can be set aside: 1. regime of heating and 2. particle size distribution. By controlling these parameters, it is possible to achieve optimal results in the production of glass-ceramics of FFW RTB Bor.

It is determined that phase composition of FFW consists of fayalite (40 %), magnetite (25 %) and glass (35 %), which is an important basis for the glass-ceramics production.

Two intervals of sintering is observed as a consequence of the different reaction rate and different sizes of particles.

Heating regime of 29ºC/min is determined as optimal because the liquid phase is being developed and penetrated into inter - granular space fast enough. The process of sintering ends within 5.2 min with minimal energy and time consumption.

Kinetics of liquid phase development during the FFW sintering highly depends on grain size distribution. Hence, by the selection of particle size distribution kinetics of sintering can be predicted.

Glass-ceramics made of hematite and glassy phase were obtained by sintering the pressed glass frit of FFW.

By changing the heat treatment conditions the microstructure and properties of the final product can be controlled.

This study marks the beginning of a more comprehensive examination which will include other modes of sintering. Further, it will be possible to add small grains of aggregate that would act as reinforcement bars, while the FFW will be a binder.

Acknowledgements

5. References

1. W. Davenport, M. King, M. Schlesingr, A.K. Biswas, Extractive metallurgy of copper, Chapter 4, Pergamon, USA 2002.
2. R. Stanojlović, Z. Stirbanovic J. Sokolovic, JMM, 44 (2008) 44 – 50.
3. M. Cocic, Application of the flotation waste from the RTB Bor for glass – ceramics. PhD thesis, Faculty of Mining – Geology, University of Belgrade, Belgrade, 2012.
4. G. Bogdanovic, M. Trumic, Maja Trumic, D. Antic, ROR, 4 (2011) 37–43.
5. M. Dimitrijevic, A. Kostov, V. Tasic, N. Milosevic, J. Hazard. Mater., 164 (2009) 892-899.
6. A. Karamanov, M. Aloisi and M. Pelino, J. Hazard. Mater., 140 (2007) 333–339.
7. S. Coruh, O. Nuri Ergun and T. Cheng, Waste Manage. Res., 24 (2006) 234-241.
8. M. Pelino, Waste Manage., 20 (2000) 561–568.
9. I. Alp, H. Deveci, H. Sungun, J. Hazard. Mater., 159 (2008) 390–395.
10. B. Gorai, R. K. Jana, Premchand, Resour. Conserv. Recy., 39 (2003) 299–313.
11. P. Asokana, M. Saxena, S.R. Asolekar, J. Hazard. Mater., 137 (2006a) 1589–1599.
12. P. Asokana, M. Saxena, S.R. Asolekar, Sci. Total. Environ., 359 (2006b) 232–243.
13. P. Asokana, M. Saxena, S.R. Asolekar, Mater. Charact., 61 (2010) 1342–1355.
14. S. Ju, Yifei Zhang, Yi Zhang, P. Xue, Y. Wang, J. Hazard. Mater., 192 (2011) 554–558.
15. M. Romero and J. Ma. Rincon, J. Eur. Ceram. Soc., 18 (1998) 153–160.
16. P. Asokana, M. Saxena, S.R. Asolekar, Build. Environ., 42 (2007) 2311–2320.
17. W. Shuming, Z. Caixing, C. Jundan, J. Mater. Sci. Technol., 30 (2014) 1208-1212.
18. H. Aripin, S. Mitsudo, B. Rahmat, S. Tani, K. Sako, Y. Fujii, K. Kikuchi, T. Saito, T. Idehara, S. Sabchevski, Sci Sinter., 46 (2014) 55-64.
19. G. Scarinci, G. Brusatin, L. Barbieri, A.Corradi, I. Lancellotti, P. Colombo, S. Hreglich and R. Dalligna, J. Eur. Ceram. Soc., 20 (2000) 2485–2490.
20. P. Colombo, G. Brusatin, E. Bernardo, G. Scarinci, Curr. Opin. Solid St. M., 7 (2003) 225–239.
21. R. D. Rawlings, J. P. Wu, A. R. Boccaccini, J. Mater. Sci., 41 (2006) 733-761.

22.D. W. Kingery, Introduction to Ceramics, J.Wiley&Sons, Inc., New York, 1960.
23.M. E. Fleet, Acta Crystallogr. B, 37 (1981) 917-920.
24.R. S. Joseph, Am. Mineral., 60 (1975) 1092-1097.
25.E. N. Maslen, V.A. Streltsov, N.R. Streltsova, N. Ishizawa, ASBSD, 50 (1994) 435-441.
26.A. Fluegel, J. Am. Ceram. Soc., 90 (2007a) 2622-2625.
27.A. Fluegel, Glass Technol-Part A, 48 (2007b) 13–30.
28.A. Kucuk, A. G. Clare, L. Jones, Glass Technol. 40, (1999) 149-153.

Садржај: *У екстракцији бакра, посебно у процесу флотацијског обогаћивања и пирометалуршке прераде настају отпадни материјали који представљају велике загађиваче животне средине. Да би се размотрила применљивост дефинитивне флотацијске јаловине за производњу нових материјала из групе стакло-керамике поред елементарног, фазног и минералног састава, испитане су и термичке особине. У раду је испитана кинетика синтеровања дефинитвне флотацијске јаловине (настале у процесу флотације топионичке шљаке) при различитој динамици загревања ($1^oC/min$, $29^oC/min$ и $43^oC/min$), како би се нашли оптимални услови при којима синтеровање може да се спроведе без деформације тела и са минимумом утрошка енергије и времена. Резултати указују на економичнију производњу материјала из групе стаклокерамике при синтеровању са режимом грејања од $29^oC/ min$.*
Кључне речи: *дефинитивна флотацијска јаловина, кинетика синтеровања, брзина загревања, расподела величине честица, стаклокерамика.*